

## Opto-Microfluidics for Monitoring Salinity and Temperature of Sea Water

Daiying Zhang, Liqiu Men, and Qiying Chen<sup>\*1</sup>

*Department of Physics and Physical Oceanography, Memorial University of Newfoundland, St. John's, NL A1B 3X7, Canada. qiyinc@mun.ca*

### ABSTRACT

The success of ocean observation relies on effective monitoring technologies with increased functionalities, minimized size, and reduced cost, which can only be achieved through the development of new technologies. Opto-microfluidics has been increasingly recognized as powerful technologies to realize miniaturized devices for environmental monitoring, biological analyses, and chemical syntheses. By combining microfluidics and optics technologies, roomful laboratory equipment can be integrated into a palm-size chip with merits of versatile functionalities, compactness, minimized waste, and low cost. These opto-microfluidic systems are promising for applications in ocean observation.

In this study, opto-microfluidic devices for monitoring salinity and temperature of liquids are proposed and demonstrated with ultrafast laser fabrication and two-photon polymerization techniques. By applying femtosecond lasers as powerful tools to achieve laser microfabrication with unprecedented high precision and quality, a Mach-Zehnder interferometer (MZI) has been fabricated and integrated into a microchannel as a miniaturized opto-microfluidic system. When saline solution or sea water is introduced to the microchannel, different phase shifts in the MZI can be resulted, which allow determination of the salinity and temperature of the solution from output optical spectra and intensities of the MZI corresponding to different phase shifts. The sensitivities of salinity and temperature have been found to be 215.744 nm/RIU and 0.519 nm/°C for the opto-microfluidic systems developed in this study, respectively. The results demonstrate the practicability of opto-microfluidic devices for real-time salinity and temperature monitoring of sea water in harsh environment.

**Keywords:** opto-microfluidics, ocean observation, salinity, temperature

### Introduction

Temperature and salinity measurement are important parameters for monitoring ocean currents, weather, iceberg floating, and oil pollution, which are very important for fishing, ecology, navigation, and human health. Various mechanical and electronic gauges are fabricated using different techniques to achieve synchronous parameter measurements. For example, the conductivity, temperature, and depth sensor (CTD) is a popular electronic instrument to measure the physical properties of seawater [1]. The huge volume of testing equipment increases the energy consumption and cost. Optical fiber sensors to simultaneous measure temperature and salinity of seawater are reported [2-4]. The advantages of flexibility and low fabrication cost attract significant attention. However, low salinity sensitivity of fiber sensors poses a major challenge for applications. Therefore, design and fabrication of inexpensive, high-sensitive, miniaturized, and real-time sensors for oceanographic measurements are the most pressing demands.

Opto-microfluidics is a kind of novel diagnostic technique which integrates optical components and microchannels on a palm-size chip to realize one or several measurements. The significant advantages of opto-microfluidic sensors are portability, efficiency, sensitivity, versatile functionalities, compactness, minimized waste, and low cost. Opto-microfluidics has been increasingly recognized as powerful technologies to realize environmental monitoring, biological analyses, and chemical syntheses.

In this paper, we report a waveguide-Mach-Zehnder interferometer (MZI) based opto-microfluidic device for simultaneous monitoring temperature and salinity of seawater. By applying femtosecond lasers microfabrication in the photoresist material, a Mach-Zehnder interferometer (MZI) has been fabricated and integrated into a microchannel as a miniaturized opto-microfluidic system. When saline solution or sea water is introduced to the microchannel, different phase shifts in the MZI can be induced, which allows determination of the salinity and temperature of the solution from output spectra and light intensities of the MZI corresponding to different phase shifts.

**Materials and Methods**

Figure 1 illustrates a typical microfabrication system with a femtosecond laser which is used in this study. The Ti: sapphire femtosecond laser with wavelength and repetition rate of 800 nm and 80 MHz, respectively, is focused on a sample by an objective lens (20×, 0.46 NA). A variable attenuator, consisting of a half wave plate and a polarizer, is placed in the path of the beam to control and continuously adjust the output power of the laser. A shutter triggered by a computer program is used to control the exposure time of the sample to laser irradiation. A power meter monitors the change of the laser power in real time through a beam splitter. A glass substrate covered with dried photoresist material SU-8 (Microchem®) is placed on the XY motion stages. By moving the translation stages (X, Y, Z directions) programmed by the computer, thereby adjusting the focal points in 3D, the desired features are fabricated. After exposure by the laser, a development process is used to wash away any unhardened material with one or more solvents (generally ethanol), leaving only the created microstructures on the substrate (Figure 2).

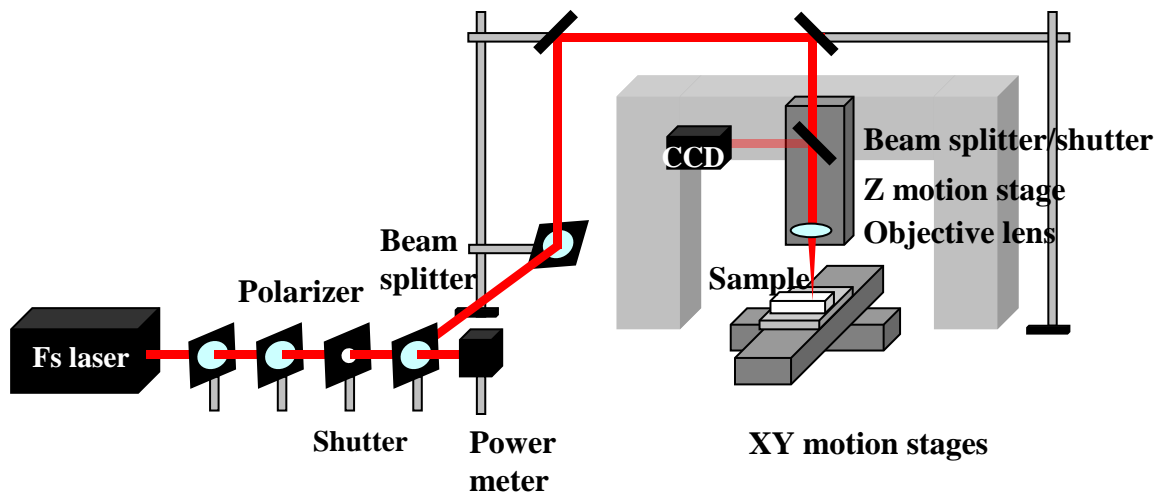


Figure 1 Schematic illustration of a microfabrication system with a femtosecond laser

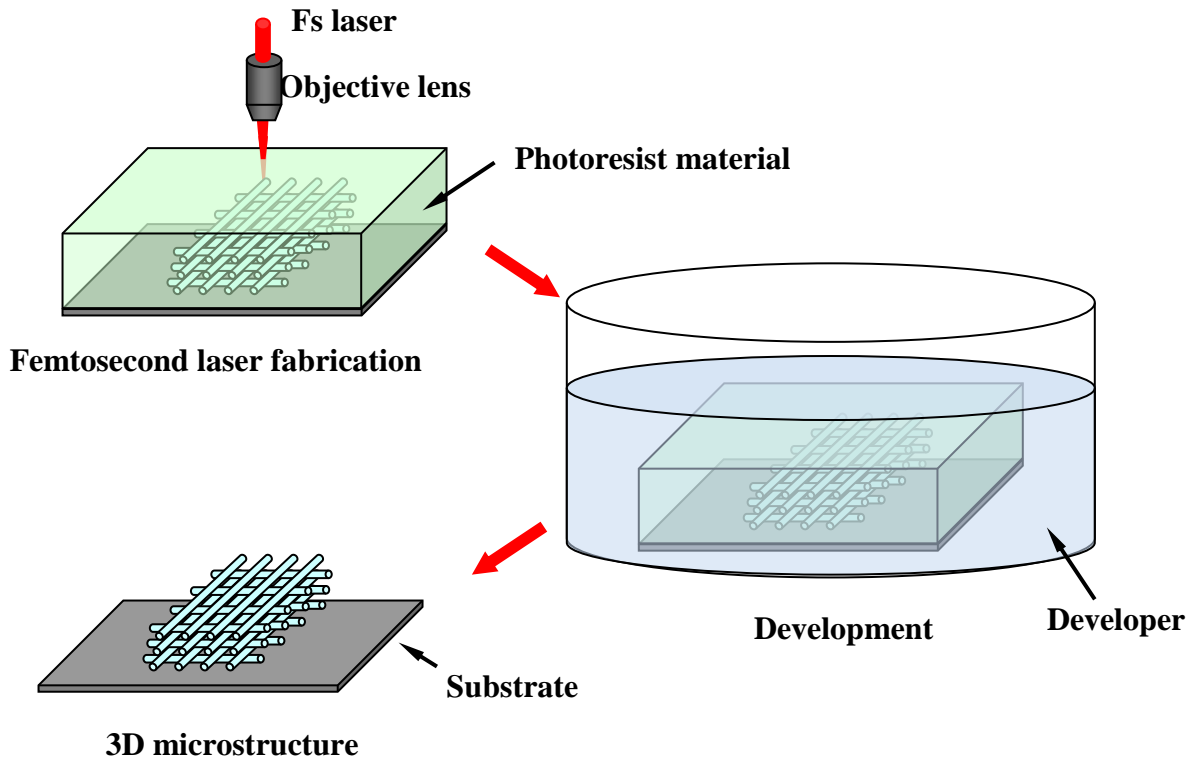


Figure 2 Schematic illustration of 3D microfabrication with two-photon polymerization technique

Mach-Zehnder interferometer (MZI) is a device to detect the relative phase shift variation between two beams which are usually split from a single source. In opto-microfluidic devices, a MZI structure is typically integrated into an optical waveguide as shown in Figure 3. The signal is first coupled into the waveguide, and then split into two arms. One arm is a reference arm to compare the phase difference, and the other arm is used to sense the phase changes due to the variation of surround environmental parameters such as temperature [5,6], concentration [7,8], and refractive index [9].

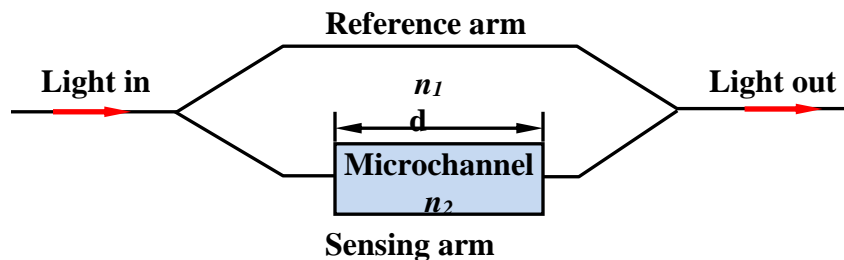


Figure 3 Schematic illustration of an opto-microfluidic MZI

The output light intensity can be expressed as follow:

$$I = I_1 + I_2 + 2\sqrt{I_1 I_2} \cos(\delta\varphi) \quad (1)$$

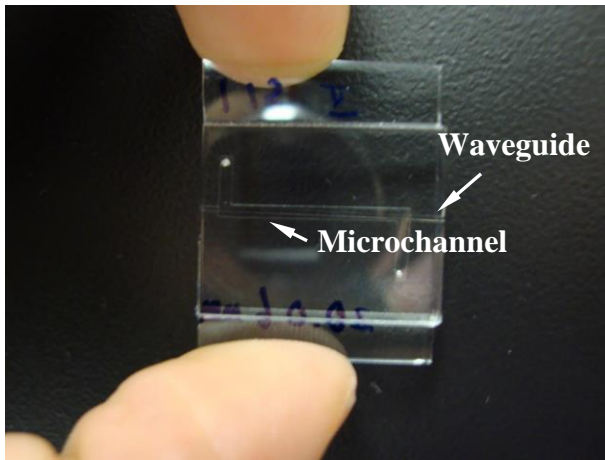
where  $I$  is the output intensity,  $I_1$  and  $I_2$  are the beam intensities, and  $\delta\varphi$  is the phase difference of the two beams.

The phase difference is

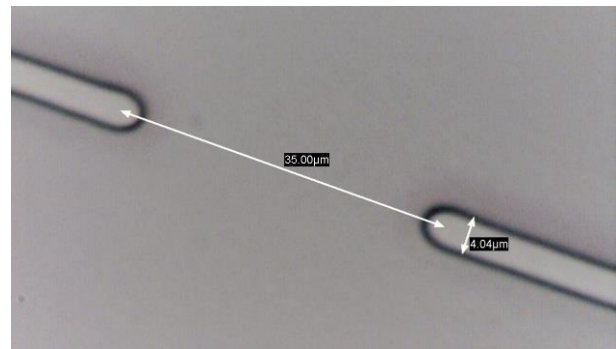
$$\delta\varphi = \frac{2\pi(n_1 - n_2)d}{\lambda} \quad (2)$$

where  $d$  is the length of the microchannel,  $\lambda$  is the light wavelength,  $n_1$  and  $n_2$  are the refractive index of the two paths, respectively.

In this design, discontinuous cores are first produced with the photoresist of SU-8 2 ( $n=1.575$  @ 1550 nm) by femtosecond laser, then the cladding is exposed with the photoresist of SU-8 3050 ( $n=1.55$  @ 1550 nm) by UV light. A Polydimethylsiloxane (PDMS) layer with a microchannel covers the substrate as shown in Figure 4. A taped SMF couples the light into the core. When beams transmit into the gap from the core, part of light is recoupled into the core, and the other part is scattered into cladding (Figure 5). If the size of core is smaller than the core diameter of the single-mode fiber (10.0  $\mu\text{m}$  corning® SMF-28e), a SMF is used to collect the light comes out from the core and the cladding to generate interference. The length of the gap between the cores is  $l_g$  and the sensing arm is  $d$ . Figure 5 (b) presents a near field image of the transmission light in which the bright dot in the middle is the light comes from the core, while the long bright line is the light comes from the cladding.



(a)



(b)

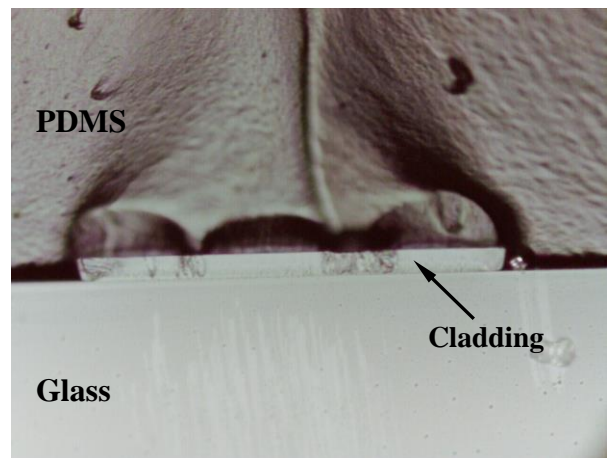
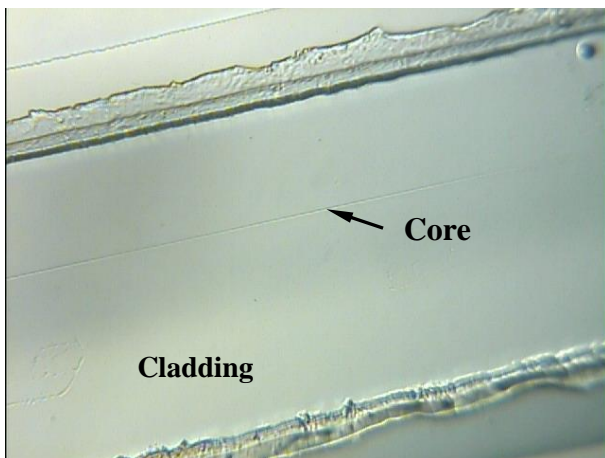


**Figure 4** (a) A photo of a waveguide-MZI based opto-microfluidic chip. (b) A photo of discontinuous cores with a gap length of 35  $\mu\text{m}$ . (c) Waveguide structure. (d) Cross section of the chip.

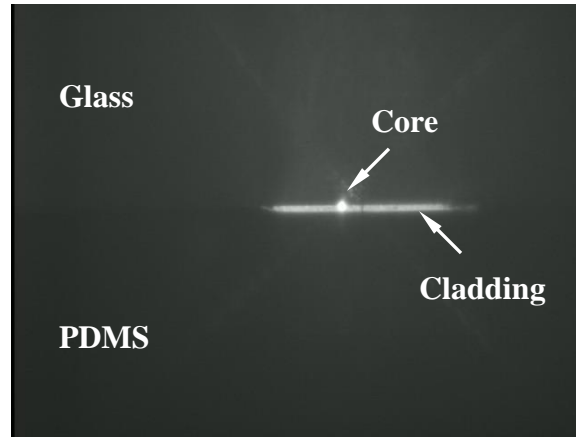
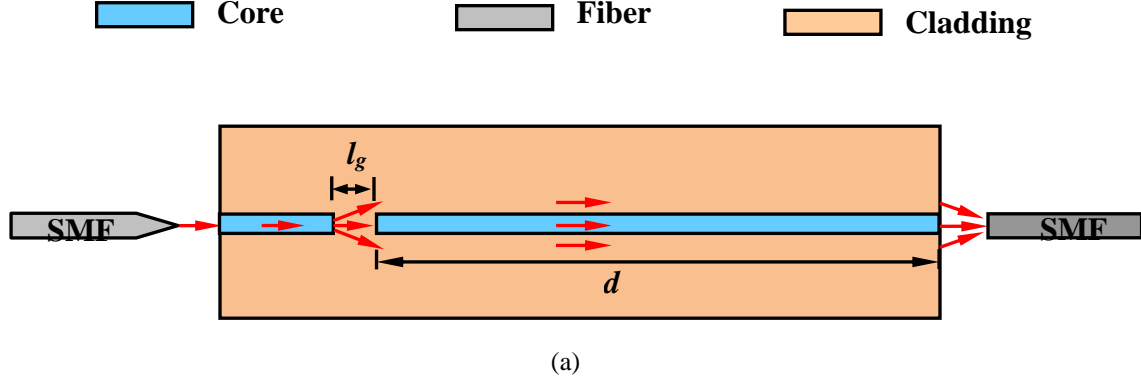


**Figure 5** (a) Schematic of MZI with symmetrical core. (b) The near field image of the transmission light.

In this case, the Equation (2) changes to

$$\delta\varphi = \frac{2\pi(n_{eff-co} - n_{eff-cl})d}{\lambda} = \frac{2\pi\Delta n_{eff}d}{\lambda} \quad (3)$$

where  $n_{eff-co}$  is the effective RI of the core,  $n_{eff-cl}$  is the effective RI of the cladding,  $\Delta n_{eff}$  is the RI difference of core and cladding, and  $d$  is the length of the chip.

When the phase difference satisfies the condition:

$$\delta\varphi = 2m\pi \quad (4)$$

where  $m$  is the order of the MZI, the attenuation peak or valley wavelength  $\lambda_m$  can be expressed

as:

$$\lambda_m = \frac{\Delta n_{eff}d}{m} \quad (5)$$

Liquids with different RIs can be injected into the microchannel. As a result, the effective refractive index of the cladding varies accordingly. However, the effective refractive index of the SU-8 core is hardly affected by the liquid. Therefore, Equation (5) can be shown as:

$$\delta\lambda_{m,n} = \lambda_{m,n'} - \lambda_{m,n} = \frac{(\Delta n_{eff,n}d + \delta n_{eff,n}l)}{m} - \frac{\Delta n_{eff,n}d}{m} = \frac{\delta n_{eff,n}l}{m} = \frac{\delta n_{eff,n}\lambda}{\Delta n_{eff,n}} \frac{l}{d} \quad (6)$$

where  $\delta n_{eff,n} = n'_{eff-cl} - n_{eff-cl}$ ,  $d$  is the length of the chip, and  $l$  is the length of the microchannel.

If the environmental temperature of the waveguide rises, both the effective refractive indices of the cladding (SU-8-3050) mode and the core (SU-8 2) mode change to different extents ( $\delta n_{eff,T}$ ) due to the fact that SU-8-3050 and the SU-8 2 are made of different solvents. The attenuation peak wavelength shift  $\delta\lambda_{m,T}$  is:

$$\delta\lambda_{m,T} = \lambda_{m,T'} - \lambda_{m,T} = \frac{(\Delta n_{eff,T} + \delta n_{eff,T})d}{m} - \frac{\Delta n_{eff,T}d}{m} = \frac{\delta n_{eff,T}d}{m} \quad (7)$$

where 
$$\delta n_{eff,T} = \left( \frac{dn}{dT}_{core} - \frac{dn}{dT}_{cladding} \right) T$$

$dn/dT$  is the thermo-optic coefficient of the material.

Therefore, the shift in the peak wavelength can be expressed as:

$$\delta\lambda_{m,T} = \frac{\left( \frac{dn}{dT}_{core} - \frac{dn}{dT}_{cladding} \right) d}{m} T = \frac{\left( \frac{dn}{dT}_{core} - \frac{dn}{dT}_{cladding} \right) \lambda}{\Delta n_{eff,T}} T \quad (8)$$

## Results and Discussion

A chip with a gap length of 200  $\mu\text{m}$  is used to simultaneous sense the refractive index and temperature of the saline solution. The core size is 4.15  $\mu\text{m} \times 3.20 \mu\text{m}$ , and the cladding size is 9.88  $\mu\text{m} \times 125 \mu\text{m}$ . The sensing arm is 24.29 mm and the length of the microchannel is 16.00 mm. Figure 6 shows the transmission spectrum with salient interference patterns. The chip is first placed on a small hotplate, and heated gradually. Transmission spectra are recorded and compared. Figure 7 presents the peak shift (red shift) at different temperatures. The temperature sensitivity is 0.519 nm/ $^{\circ}\text{C}$ . Keeping the temperature of hotplate at 35 $^{\circ}\text{C}$ , saline solutions are infused into the microchannel one by one. Figure 8 shows the dependence of the peak shift on refractive index /salinity. The salinity sensitivity is -215.744 nm/RIU.

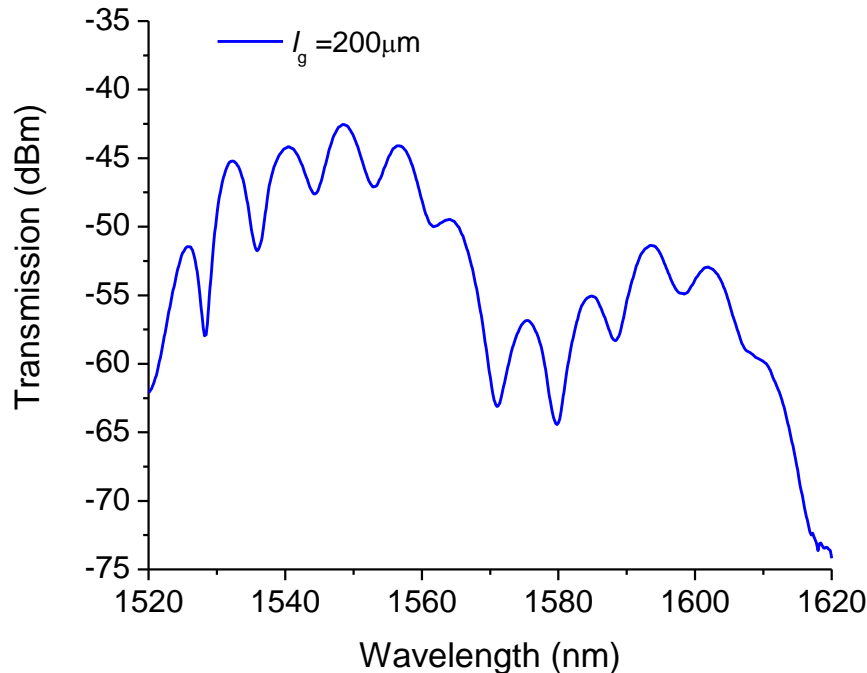


Figure 6 Transmission spectrum at the room temperature.

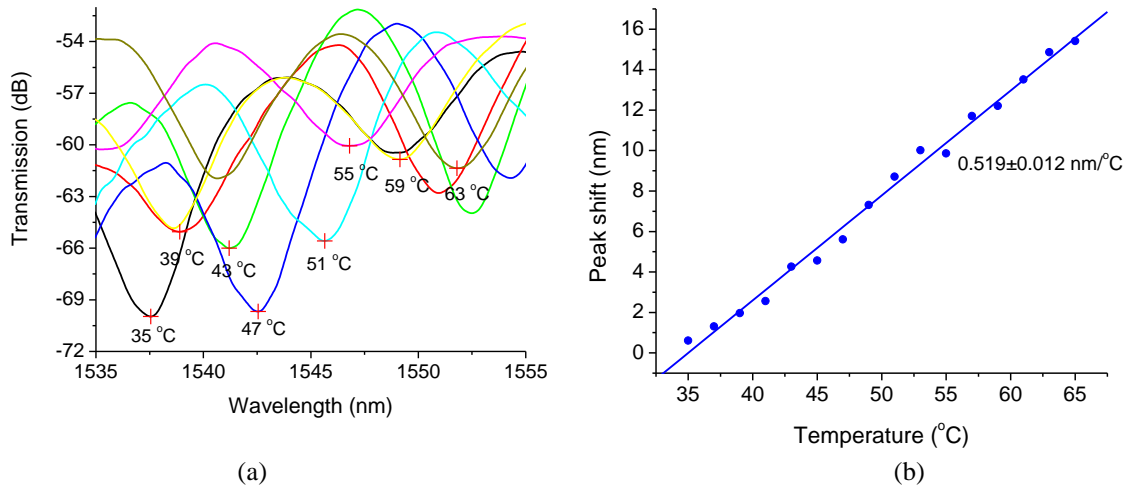


Figure 7 (a) Transmission spectra at different temperatures. (b) Dependence of the peak shift on temperature.

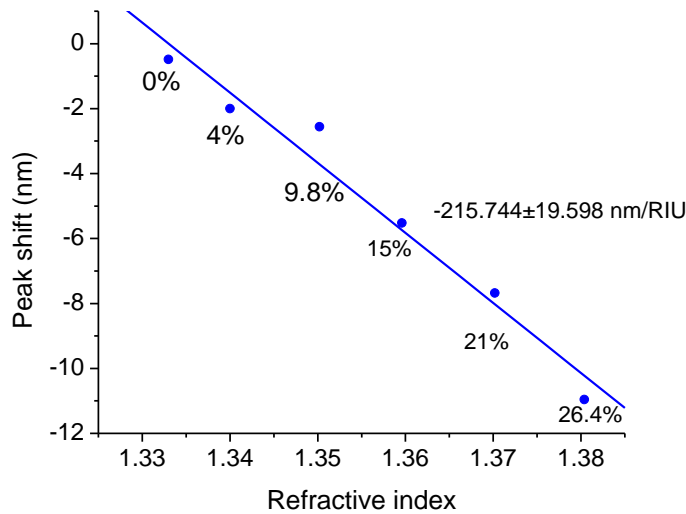


Figure 8 Dependence of the peak shift on refractive index/salinity.

In the case of simultaneous variations in both temperature and salinity, the total wavelength shift can be expressed as:

$$\Delta\lambda = 0.519\Delta T - 215.744\Delta n$$

where  $\Delta T$  is the change of the temperature, and  $\Delta n$  is the change of the refractive index.

In order to prove the validity of the chip, water samples are applied to the chip: melted iceberg water, pond water, and seawater. Distilled water is first infused into the chip for reference, and

then water samples are injected into the microchannel. Figure 9 describes the experimental results. The RI of iceberg is about 1.3347 which is a bit higher than DI water which is caused by the contamination of the sea water. The RI of the pond is 1.3360. The RI of seawater is about 1.3393. By calculation [10], the salinity is about 32.578‰ which is reasonable for the seawater.

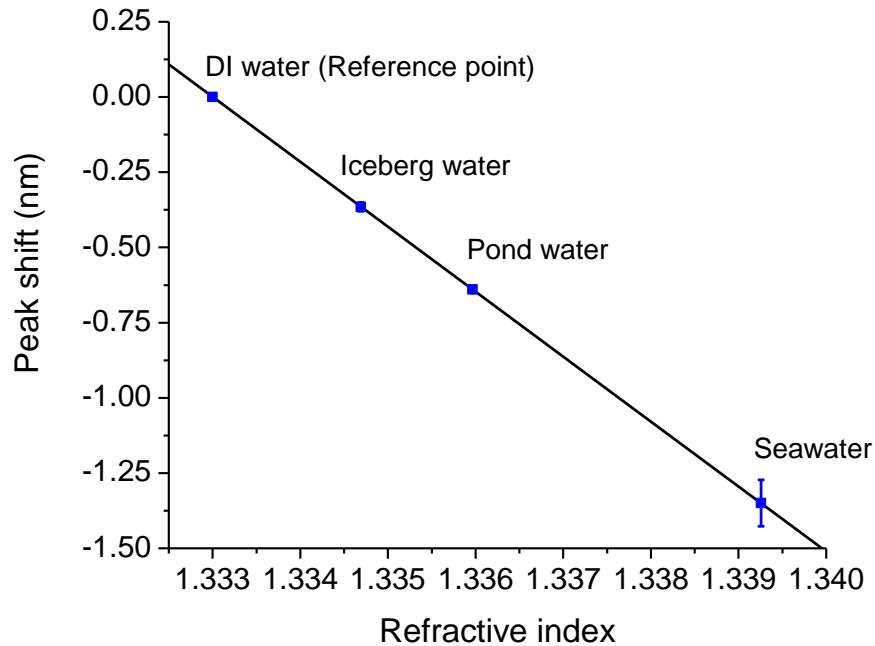


Figure 9 Refractive index measurements for different water samples.

## Conclusions

In summary, we have successfully designed and fabricated an opto-microfluidic MZI sensor based on waveguide with discontinuous core. Simultaneous sensing of temperature and refractive/salinity of salt solutions has been achieved. The temperature and refractive index sensitivities are 0.159 nm/°C and -215.744 nm/RIU which are much higher than these of fiber sensors (0.0102 nm/°C and 0.0165 nm/M in Ref.2, 0.029 nm/°C and 0.069 nm/ppt in Ref.4). Different water samples are tested using this chip with good agreement, which demonstrates the practicability of opto-microfluidic devices for *in situ* monitoring salinity and temperature of sea water with high sensitivities and low cost.

## Acknowledgement

The authors thank Natural Sciences and Engineering Research Council of Canada (NSERC), Canada Research Chairs Program, Canada Foundation for Innovation, the Province of Newfoundland and Labrador, and the Memorial University of Newfoundland on the support of research infrastructure.

## References



## Joint Conferences:

The 2014 Annual Conference of the International Society for Environmental Information Sciences (ISEIS)

The 2014 Atlantic Symposium of the Canadian Association on Water Quality (CAWQ)

The 2014 Annual General Meeting and 30th Anniversary Celebration of the Canadian Society for Civil Engineering Newfoundland and Labrador Section (CSCSE-NL)

The 2nd International Conference of Coastal Biotechnology (ICCB) of the Chinese Society of Marine Biotechnology and Chinese Academy of Sciences (CAS)



1. Lawson K. and Larson N. G. (2001). CTD. In: Steele J. H., Thorpe S. A., Turekian K. K. (eds.), *Encyclopedia of Ocean Sciences: Vol 1*. Academic Press Inc Publishing, PP. 579-588.
2. Men L., Lu P., and Chen Q. (2008). A multiplexed fiber Bragg grating sensor for simultaneous salinity and temperature measurement. *J. Appl. Phys.*, 103(5), 053107.
3. Choi H.Y., Mudhana G., Park K.S., Peak U.C., and Lee B.H. (2010). Crosstalk free and ultra-compact fiber optic sensor for simultaneous measurement of temperature and refractive index. *Opt. Express*, 18(1), 141–149.
4. Nguyen L.V., Vasiliev M., and Alameh K. (2011). Three-wave fiber Fabry–Pérot interferometer for simultaneous measurement of temperature and water salinity of seawater. *IEEE Photo. Tec. Lett.*, 23(7), 450-452.
5. Wang Y., Yang M., Wang D.N., Liu S., and Lu P. (2010). Fiber in-line Mach–Zehnder interferometer fabricated by femtosecond laser micromachining for refractive index measurement with high sensitivity. *J. Opt. Soc. Am. B*, 27(3), 370-374.
6. Dumais P., Callender C. L., Noad J.P., and Ledderhof C. J. (2008). Integrated optical sensor using a liquid-core waveguide in a Mach-Zehnder interferometer. *Opt. Express*, 16(22), 18164-18172.
7. Crespi A., Gu Y., Ngamsom B., Hoekstra H.J.W.M., Dongre C., Pollnau M., Ramponi R., Vlekkert H.H., Watts P., Cerullo G., and Osellame R. (2010). Three-dimensional Mach-Zehnder interferometer in a microfluidic chip for spatially-resolved label-free detection. *Lab Chip*, 10(9), 1167-1173.
8. Lapsley M.I., Chiang I.K., Zheng Y.B., Ding X., Mao X., and Huang T.J. (2011). A single-layer, planar, optofluidic Mach–Zehnder interferometer for label free detection. *Lab Chip*, 11(10), 1795-1800.
9. Densmore A., Xu D.X., Janz S., Waldron P., Mischki T., Lopinski G., Delâge A., Lapointe J., Cheben P., Lamontagne B., and Schmid J.H. (2008). Spiral-path high-sensitivity silicon photonic wire molecular sensor with temperature-independent response. *Opt. Lett.*, 33(6), 596-598.
10. Quan X. and Fry E. S. (1995). Empirical equation for the index of refraction of seawater. *Appl. Opt.*, 34(18), 3477–3480.